Heliyon 9 (2023) e17943

Contents lists available at ScienceDirect

Heliyon

journal homepage: www.cell.com/heliyon

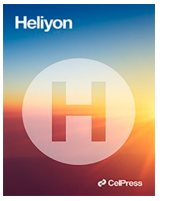

Comparative study of the combustion, pyrolysis and gasification processes of *Leucaena leucocephala*: Kinetics and gases obtained

S. Clemente-Castro [a], A. Palma [a,*], M. Ruiz-Montoya [a], I. Giráldez [b], M.J. Díaz [a]

[a] *Department of Chemical Engineering, Physical Chemistry and Materials Science. Pro²TecS – Product Technology and Chemical Processes Research Centre. University of Huelva, Campus "El Carmen", Spain*

[b] *Department of Chemistry "Prof. José Carlos Vílchez Martín". Pro²TecS – Product Technology and Chemical Processes Research Centre. University of Huelva, Campus "El Carmen",Spain*

ARTICLE INFO

Keywords:
Leguminous
Biofuel
Pyrolysis
Gasification
DAEM method
TD-GC/MS

ABSTRACT

Leucaena leucocephala is a fast-growing leguminous biomass with great energetical and value-added chemical compounds potential (saccharides, biogas, bio-oil, etc.). Using the thermogravimetric and derivative thermogravimetric curves, the different trends followed by L. leucocephala during pyrolysis, 0.25 equivalence ratio (ER) of gasification, 0.50 equivalence ratio of gasification and combustion were analyzed, and the activation energies were obtained by Distributed Activation Energy Model (DAEM) method. Gas samples were collected through adsorption tubes during the gasification at 0.25 ER and 0.50 ER to observe the distribution of the main chemical products in this process by gas chromatography/mass spectrometry and were compared with pyrolysis products. It was found that small amounts of oxygen have changes in the kinetics of the process, leading to significant decreases in the activation energy at the beginning of the degradation of components such as cellulose (from 170 to 135 kJ mol^{-1} at 0.25 conversion at 0.50 ER gasification). The activation energy of lignin disintegration was also reduced (342 kJ mol^{-1}), assimilating the beginnings of gasification processes such as the Boudouard reaction. 0.50 ER gasification is potentially an interesting process to obtain quality bio-oil, since a large amount of hexane is detected (44.96%), and value-added oxygenated intermediates such as alcohols and glycols. Gasification at 0.25 ER, on the other hand, is much more similar to pyrolysis, obtaining a wide variety of short-chain compounds resulting from the disintegration of the main lignocellulosic components, especially ketones such as 1-hydroxypropan-2-one (19.48%), and notable amount of furans and anhydrosugars like d-allose (5.50%).

1. Introduction

It is estimated that the human industrial activity has increased global temperature by around 0.2 °C per decade, which in 2017 was between 0.8 and 1.2 °C, over pre-industrial revolution levels. The Intergovernmental Panel on Climate Change (IPCC) demonstrated that even fulfilling the current promises of the Paris agreement, the temperature will continue to rise with severe consequences for ecosystems and the lives of people [1]. The need to drastically reduce the emission of greenhouse gases is fully accepted, reducing 25% in 2030 would be below 2 °C pre-industrial, but the ultimate goal is net zero emissions. To achieve this goal, a change in society must be

* Corresponding author. Department of Chemical Engineering, Physical Chemistry and Materials Science. Pro²TecS – Product Technology and Chemical Processes Research Centre. University of Huelva, Spain.
E-mail address: alberto.palma@diq.uhu.es (A. Palma).

https://doi.org/10.1016/j.heliyon.2023.e17943
Received 27 March 2023; Received in revised form 27 June 2023; Accepted 3 July 2023
Available online 6 July 2023

proposed, especially in the energy sector, which continues to be supplied mostly by fossil fuels, although it is already turning to innovate to develop an increasingly clean sector [2]. One of the routes with the most potential to generate energy in a sustainable system is the use of biomass as a substitute for traditional fossil fuels. Even though the sustainability of the consumption of first-generation biomass (traditional crops) is highly criticized due to problems of deforestation, abusive use of water and pollution [3], second-generation biomass (forestry, agricultural and urban organic fraction or industrial waste) has a good availability of feedstock with a very low carbon impact and sulfur content [4]. The energy potential of second-generation biomass is high and could represent a significant fraction in the global energy mix, which is estimated that it was 53 EJ for the year 2018 [5].

The use of biomass directly as biofuel presents serious complications being its high humidity, oxygen content, low calorific value and high variable in composition and properties, some of the major issues [6]. However, the application of thermochemical treatments to convert biomass into products that are easier to process is an appropriate path to avoid this awkwardness. The goal of thermochemical treatments of biomass is to minimize unwanted by-products by optimizing process parameters [7]. Heat and specific chemical alterations are applied to biomass to generate biofuels with a higher quality and energy density than the direct use of biomass itself [8]. The main thermochemical processes to convert biomass into quality biofuels are torrefaction, combustion, pyrolysis and gasification [9]. Torrefaction is a process that concerns a moderate pyrolysis of biomass at not excessive temperature (200–300 °C) which partly degrades the lignocellulosic components while removing water and some more susceptible volatile organic compounds, generating a biochar similar to fuel coal [10]. Pyrolysis is a high temperature process (250–600 °C) under inert conditions that allows biomass to be converted into three fractions: bio-liquid, biochar and biogas, which can be used to produce energy including derivate products of the chemical industry [11]. Heat and electricity are the result of the combustion of biomass, the most widespread thermochemical process in the industry, although the large amount of CO_2 and NO_2 in real process must be considered, there are even studies that indicate that carbon dioxide debt could be highly dependent on the relationship between burning and reforestation intensity [12]. Gasification is an emerging thermochemical process that operates in the presence of an oxidating atmosphere to produce synthesis gas ($CO + H_2$) and far fewer dangerous products such as particles, mercury, NO_x, SO_x and CO_2, among many others [13]. The parameter that most influences the gasification process is the equivalence ratio (ER) defined as the relationship between the oxygen or air that is fed to the process and that necessary for the complete oxidation of the matter, normally industrial gasifiers feed oxygen between 0.1 ER and 0.5 ER to control the quality of the generated gas [14]. An alternative that is spreading and that improves the nature of bio-oil overcoming various barriers in traditional treatments is the application of co-thermochemical conversions of lignocellulosic materials and fossil feedstocks [15].

Owing to the intricacy of the thermochemical processes of biomass conversion, it is hard to define the kinetics of this reactions and anticipate the formation of bioproducts adequately, therefore, designing and optimizing these processes is an arduous task [16]. A very useful tool for the research and understanding of the kinetic behaviour of these processes is thermogravimetric analysis (TGA) which the loss of mass during the increase in temperature due to the decomposition processes is measured. There are numerous kinetic models to use the numerical data obtained by TGA as model-fit or model-free, however, although these models have been contrasted for highly heterogeneous reactions, kinetic models, among those which attract attention the activation energy distribution model (DAEM) to study biomass kinetic parameters, are comparatively better [17]. In DAEM approach, it is considered that distinct first-order reactions with an irreversible component are occurring concurrently during the thermal process of sample destruction in consequence it is a method that is closer to reality since it does not consider a single first-order reaction like typical kinetic methods [18]. These considerations are very useful when studying different thermochemical processes as in this study, and it is the reason why the distributed activation energy model (DAEM) method is used for kinetic analysis.

Regarding biomass, in recent years, leguminous have gained relevance as an environmentally friendly alternative to typical fast-growing biomasses such as eucalyptus, willow or poplar by virtue of its great capacity for nitrogen fixation, recovery of contaminated soils and reforestation without absorbing so many water resources and care. As the most representative leguminous, this study chose *Leucaena leucocephala*, a fast-growing tree native to Mexico that was introduced in other areas of the world mainly Australia as an agroforestry crop for fodder, fuel and timber requirements [19]. This leguminous stimulates nitrogen fixation in consequence of synergies with bacterial microorganisms of the variety Rhizobium. In areas where the vegetarian does not grow or very little due to the poor conditions of metals in the soil, *L. leucocephala* has been used as revegetation biomass with good results [20,21].

Thermal desorption combined to gas chromatography-mass spectrometry (TD-GC/MS) is a frequently procedure for the inquiry of organic volatiles compounds from gaseous samples [22]. Therefore, GC/MS is used to analyze the gas products which can avoid secondary reactions between products highly reactive [23]. Likewise, the reactions mechanisms of pyrolysis-derived products such as char with CO_2 gasification treatments were studied by TG-FTIR-GC-MS [24].

The aims of the article are to compare three thermal treatments (pyrolysis, gasification and combustion) of*Leucaena leucocephala*, a common leguminous biomass, from the kinetic perspective with the help of thermogravimetric analysis (TGA). The DAEM kinetic method has been employed to accurately calculate kinetic parameters. Gasification of L. *leucocephala*was conducted using 0.25 and 0.50 equivalence ratios of stoichiometric oxygen to identify key compounds and evaluate the potential of industrial products. These equivalence ratios are within the range of operation for industrial gasifiers.

2. Materials and methods

2.1. Samples preparation and analysis

L. leucocephala samples were obtained from a specific crop in Campus La Rabida cultivated by the agroforestry group of the University of Huelva (Huelva, Spain). The harvested wood was stored and soon after reduced its moisture content to less than 8 wt%

and then chopped to pieces between 2 cm × 0.5 cm. The fragments of woody, branches and twigs were separated from leaves and non-woody components previously to crush in a hammer mill to chips with a particle diameter of 0.5–5 mm according to standard Tappi T-257 [25], which was the particle size of the thermogravimetric experiment.

The ultimate analysis of *L. leucocephala* was carried out applying the CHN method described in the ASTM D5373-02 method. The elementary distribution of carbon, oxygen, hydrogen, nitrogen and sulfur in the biomass was 47.3, 41.6, 6.1, 1.9 and 0.1% respectively, determined by the Higher Council of Scientific Research (CSIC) of Seville using an elemental analyzer (Leco TruSpec CHN) and Eltra Helios CHS (University of Huelva). The empirical formula of *L. leucocephala* is $CH_{1,548}O_{0,661}N_{0,034}S_{0,001}$. Regarding lignocellulosic analysis, samples of *L. leucocephala* were exposed to quantitative acid hydrolysis with 72% sulfuric acid following TAPPI T-249 cm-85 [26], solid residue was recovered to measure Klason lignin resulted in 22.7%. The chemical components of *L. leucocephala* divided into carbohydrates, predominantly C_6 and C_5 sugars representing cellulose and hemicellulose; extractives; and acetyl groups, were measured by high-precision liquid chromatography (HPLC) in hydrolysates obtaining 37.1, 18.4, 1.9 and 2.1%, respectively for the aforementioned compounds. The proximate analysis was carried out using a thermogravimetric analyzer following ASTM E870-82, subjecting the wood samples to pyrolysis to determine their volatile content and combustion for the ashes. Both analyses give moisture and, finally, fixed carbon was calculated by difference. The moisture of the samples was 7.03% and the volatile material, ash content and fixed carbon were 81.67%, 1.99% and 16.34% correspondingly, the latter measured on a dry basic and all this by thermogravimetry (Mettler Toledo thermogravimetry analyzer/DSC1 STARe system).

2.2. Thermogravimetric analysis

Thermogravimetric experiments applied to each of the thermochemical treatments were carried out in Mettler Toledo thermogravimetry analyzer/DSC1 STARe System. The thermogravimetric system has been previously calibrated (25–1100 °C) according to ASTM E1582-00 (Standard Practice for Calibration of Temperature Scale for Thermogravimetry). The samples of ground and well homogenized *L. leucocephala* were divided into the different alumina crucibles. The thermogravimetry equipment consists of a very high precision microbalance, an oven, thermocouples and a gas insertion system connected to a gas controller (GC 200 Mettler Toledo). In addition, the samples are automatically introduced into the oven by means of a robot.

The equivalence ratio (ER) represents the current air-biomass ratio with respect to stoichiometry and plays a key role in biomass gasification. It is probably the most crucial operating parameter for allothermal processes, since it strongly affects the composition of the gas, including tar, and its calorific value [27]. Values close to 0 correspond to pyrolysis conditions, while values equal to or greater than 1 indicate combustion conditions. Values around 0.25–0.35 appear to maximize carbon conversion and are therefore used in large-scale commercial gasification plants.

It can be expressed both as a function of the fuel air ratio and directly as oxygen as an oxidant. In the present study it has been calculated with the equivalence ratio as a function of oxygen (Eq. (1)) [28].

$$ER = \frac{\left[\frac{m_{fuel}}{m_{oxygen}}\right]}{\left[\frac{m_{fuel}}{m_{oxygen}}\right]_{st}} \tag{1}$$

in the pyrolysis, nitrogen was used as inert gas to avoid any type of secondary reaction. In the case of combustion, pure oxygen was used to ensure a more efficient oxidation reaction. And finally, for 0.25 ER and 0.50 ER gasification treatments, standard nitrogen mixtures purchased from Linde were used with substoichiometric amounts of oxygen (0.025 and 0.075 wt% in oxygen) previously calculated with the help of the elemental analysis of *L. leucocephala*. These ratios between the oxygen supplied and the biomass were chosen based on previous studies on the effect of the equivalence ratio, in which it was found that between 0.2 and 0.3 the best conversions are achieved in industrial gasifiers with a high-energy syngas product [29]. For this reason, 0.25 ER was taken as a value close to these optimums and 0.50 ER as a somewhat higher value to observe changes in kinetics and products.

Each of the sample thermochemical experiments was divided into three phases: (i) sample heating from 25 to 105 °C with an inert gas flow rate of 30 mL min^{-1} acting as a nitrogen sweep at a heating rate of 15 °C min^{-1}; (ii) kept of the temperature at 105 °C for 5 min maintaining the flow and atmosphere of the first step to ensure the loss of all the moisture in the sample; (iii) heating from 105 to 800 °C, under various heating rates (5, 10, 15, 20 and 25 °C min^{-1}) using the gas atmosphere corresponding to the desired process mentioned in the previous paragraph developing with flows of 30, 15 and 10 mL min^{-1} for pyrolysis, gasification and combustion, accordingly. The initial sample mass was in all cases approximately 10 mg and the experiments were performed in triplicate recorded the average values.

2.3. Analytical method

The DAEM method has been used to evaluate the behaviour in the pyrolysis of fossil fuels, thermal degradation of activated carbon and other complex reaction systems [30]. Some recent studies already validate the DAEM for biomass and estimated activation energies distribution of waste biomass or components thereof such as xylan and cellulose [31,32].

The DAEM is based on two assumptions: the first, a considerable amount of parallel, independent, reactions of order 1, 2 or nth with particular activation energies occur in the decomposition mechanism, and in second place, these activation energies are expressed by a continuous distribution function $f(E_a)$ [33]. Combustion, 0.25 ER gasification, 0.50 ER gasification and pyrolysis of different component of *L. leucocephala* (mainly hemicellulose, cellulose and lignin) involves many complex reactions. Therefore, it is not

accurate enough to describe thermochemical processes with a single reaction and, accordingly, DAEM method is very suitable in this study [34].

When using the DAEM method to test biomass degradation, the changes in volatile compounds, V, against time, t, are given by Eq. (2) [35]:

$$1 - V / V^* = \int_0^{\infty} \exp\left(-\frac{k_0}{\beta} \int_0^T e^{-E_a/(RT)} dT \right) f(E_a) dE_a \tag{2}$$

in whose equation V* is the initial volatile content, therefore, the ratio V/V* denotes the degree of conversion of the fuel, β is the heat rate, E_a is the activation energy, $f(E_a)$ is a distribution curve that represents the different activation energies of the reactions, and k_0 is the frequency factor of the respective activation energy. Eq. (2) can be simplified to Eq. (3) [36]:

$$V / V^* = 1 - \int_{E_s}^{\infty} f(E_a) dE_a = \int_0^{E_s} f(E_a) dE_a \tag{3}$$

The $f(E_a)$ is the normalized distributed curve of the activation energy describing the contrasts between many reactions and k_0 of each of these energies. Considering this simple model, the Arrhenius equation can be represented like this [37]:

$$ln\left(\frac{\beta}{T^2}\right) = ln\left(\frac{k_0 R}{E_a}\right) + 0.6075 - \frac{E_a}{R}\frac{1}{T} \tag{4}$$

Using Eq. (4), we can estimate activation energy through the Arrhenius equation of ln (β/T^2) vs. 1/T at the elected V/V* for different β value. Activation energies can be determined at different V/V* stages from the Arrhenius plots [38].

2.4. Volatile analysis by gasification thermal desorption GC-MS)

Gas samples were collected at the outlet of the small furnace of the thermogravimetric analyzer in the gasification processes at 0.25 ER and 0.50 ER at the temperatures which *L. leucocephala* suffered more pronounced degradation. 100 mg of TenaxR TA (117–149 μm acquired from Supelco, Bellefonte, Pennsylvania, US) prepacked in glassy frit thermal desorption (TD) tubes supplied by the same

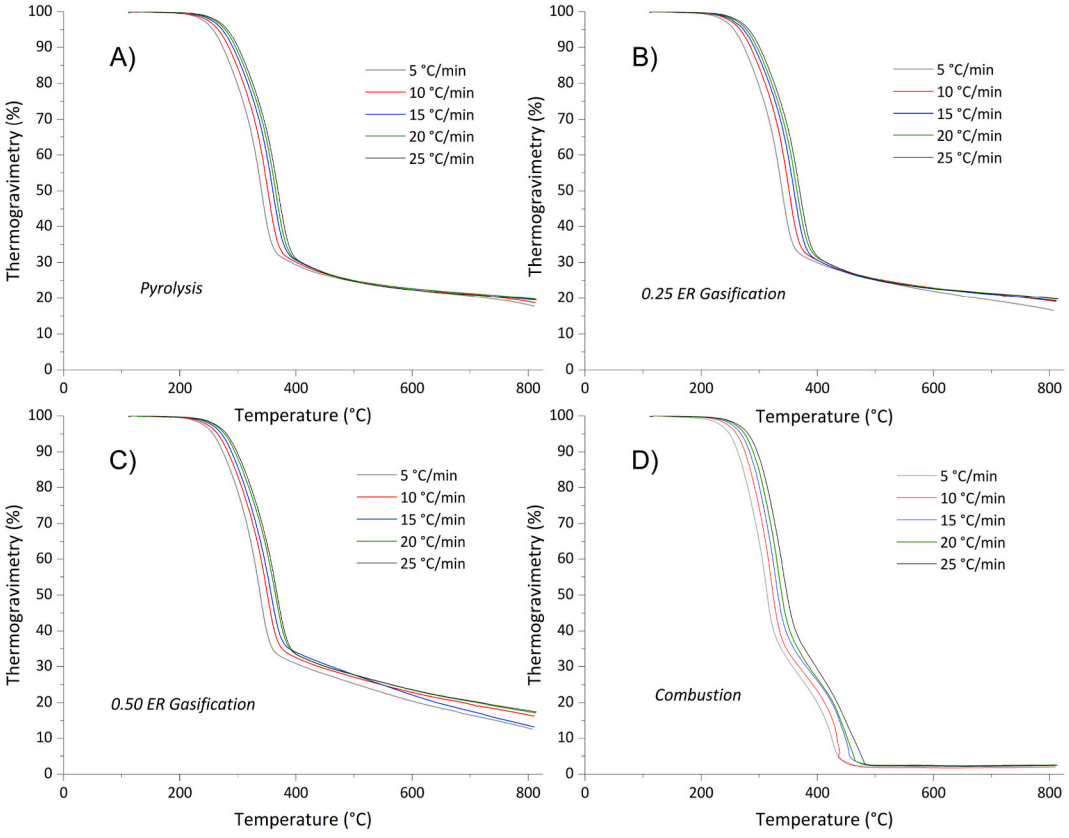

Fig. 1. Thermogravimetry curves (TGA) of differet thermochemical treatments (A) Pyrolisys, B) 0.25 ER Gasification, C) 0.50 ER Gasification and D) Combustion) applied to *L. leucocephala*.

producer (outside diameter: 6.35 mm; tube extension: 88.9 mm) and silanized glass wool, were used. Gas samples were collected for 30 s.

Tenax tube were conditioned prior to use by flushing with 50 mL min^{-1} to Helium gas at 300 °C for 15 min, after they were closed with steel plugs to prevent contamination.

TD tubes were placed into the TD autosampler to TD/GC-MS (GCMS-QP6030 Ultra, Shimadzu, Japan) for analysis. Volatile organic compounds (VOCs) were removed from a tube in the thermal desorption module (Shimadzu Thermal Desorption System TD-20, Tokyo, Japan) at 280 °C for a period of 10 min using helium as carrier gas at 50 mL/min. Then, the analytes were trapped into Tenax cold trap at −16 °C and rapidly desorbed at 280 °C during 3 min. The analytes were concentrated into head of the GC column HP-5 MS (length: 60 m, inner diameter 0.25 mm, film thickness: 0.25 μm, GC tubing: fused silica, J&W GC columns, Agilent Technologies, Santa Clara, California, US). The oven temperature program was as follows: 40 °C during 10 min, increased to at 280 °C. 1 mL/min was the flow rate of helium as carrier gas chosen in the analytical column (40, split ratio).

The mass spectrometer was executed in scan modus (42–450 *m/z*) with electron ionization (70 eV). The transfer line and ionization supply point temperatures were 250 °C and 330 °C, respectively. Volatile organic compounds were disclosed by similarity of the mass spectrum recorded by the spectrometer with the many compounds that are perfectly identified in the database of NIST 11 mass spectral library. For the control, processing and analysis of the data obtained at 0.25 ER and 0.50 ER gasification of *L. leucocephala*, Gas chromatography Mass spectrometry Postrun Analysis Software, supplied by Shimadzu Corporation (Tokyo, Japan), was the tool used.

3. Results and discussion

3.1. Thermogravimetric characteristics analysis of L. leucocephala at different thermochemical processes

3.1.1. Thermogravimetric (TG) analysis

The thermogravimetric curves of thermochemical processes applied to *L. leucocephala* were shown in Fig. 1.

As advertised in the graphs in the initial stages of the thermochemical processes there is hardly any loss of mass, but small losses begin to be elucidated around 200 °C. When temperature ramps increase, it is observed that in all cases the thermogravimetric curves shift to higher temperatures, the degree of sensitivity of this effect is very similar between different processes. When the process is located in a conversion (V/V*) of 0.5, the temperature of *L. leucocephala* at the heating rates of 5, 10, 15, 20 and 25 °C/min were 332,

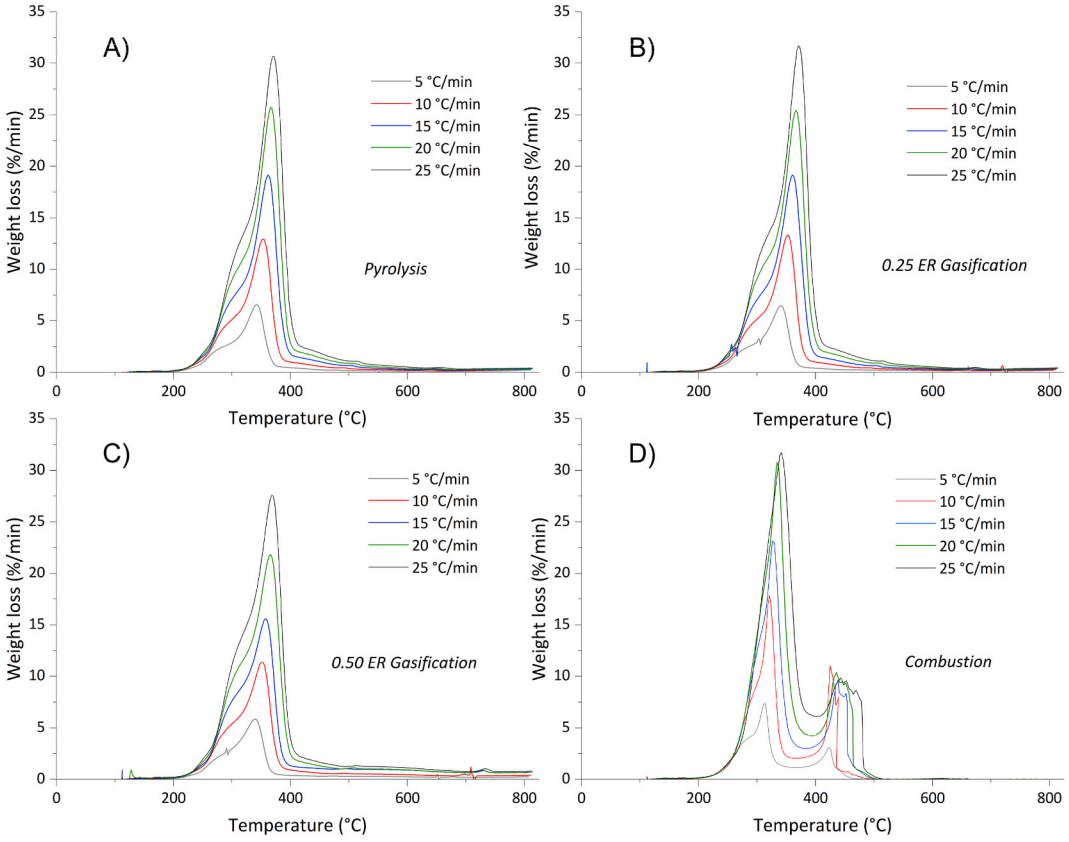

Fig. 2. Thermogravimetric derivative curves (DTG) of differet thermochemical treatmensts (A) Pyrolisys, B) 0.25 ER Gasification, C) 0.50 ER Gasification and D) Combustion) applied to *L. leucocephala*.

342, 350, 354 and 358 °C respectively, in all treatments except in the case of combustion that correspond with 314, 324, 332, 340 and 348 °C. This fact illustrates that the degradation processes of hemicellulose, cellulose and lignin in intermediate ranges are very similar in terms of mass loss with slight variations even in combustion, since this process has a higher mass destruction range cause char oxidation and the volatilization temperature at each component, is more similar than it seems at first glance.

Farther, when looking at the conversion (V/V*) range between 0.1 and 0.9, the leading temperature sections were 200–400 °C to pyrolysis (Figs. 1A), 200–450 °C to 0.25 ER gasification (Figs. 1B), 200–500 °C to 0.50 ER gasification (Figs. 1C) and 200–480 °C to combustion (Fig. 1D). Both in the pyrolysis process and in the combustion, a point of barely any mass loss is reached due to the degradation of all the volatiles and the oxidation of all the char, respectively. However, in gasifications at higher temperature degradation stages, decomposition reactions still occur, which would progress even at 800–1100 °C. The presence of evolution gases and carbon dioxide in gasification processes causes gas-char reactions, inducing a more drooping tail the more oxygen it presents in the TG curves observed in recent studies [39]. On the other hand, in combustion two slopes of the different TG curves are well differentiated (Fig. 1D) due to the existence of two typical reaction zones in combustion (degradation of volatiles and oxidation of char) [40].

3.1.2. Derivative thermogravimetry (DTG) analysis

The graphs of *L. leucocephala* DTG curves were shown in Fig. 2.

- Pyrolysis

The pyrolysis process is divided into two zones, a first stage where most of the decomposition takes place called active pyrolysis (200–400 °C) and second known as passive pyrolysis (400–700 °C) (Fig. 2A) [41].

The first zone shows two amalgamated peaks representing degradation of hemicellulose and cellulose with maximum values around 310, 315, 318, 321 and 325 °C, to 5, 10, 15, 20 and 25 °C min^{-1}, respectively referred to the hemicellulose that begins to degrade between 200 and 240 °C. As for cellulose, it degrades together with last hemicellulose and a certain amount of lignin, but it stands out in the range between 320 and 400 °C with peaks around 341, 352, 368, 366 and 370 °C, to 5, 10, 15, 20 and 25 °C min^{-1}, respectively. Observing the trend from 400 °C onwards, in the passive pyrolysis zone, the volatilization of compounds continues slightly, especially lignin, whose aromatization processes produce a slow weigh loss [42].

- **Gasification**

Gasification processes which mixtures of nitrogen with substoichiometric oxygen were used show behaviours very similar to the strictest pyrolysis. In fact, the temperature of maximum degradation of hemicellulose and cellulose were practically identical in 0.25 ER gasification and very slight differences in the case of 0.50 ER gasification regarding pyrolysis. These cellulose degradation peaks were 6.6, 13.2, 19.1, 25.6 and 31.1% min^{-1} to 5, 10, 15, 20 and 25 °C min^{-1}, respectively, in pyrolysis and 0.25 ER gasification, but these results were considerable reduced until 5.8, 11.4, 15.6, 21.8 and 27.6% min^{-1} if we talk about 0.50 ER gasification (Fig. 2B and C). This phenomenon suggests that with very low amount of oxygen there are no appreciable effects in terms of the degradation of component in the active zone, although when the oxygen supply begins to be higher, small changes initiate to be observed. It is decisive in certain surface reactions, changing the dynamics of the process into more complex char gasification [43]. At the end of both gasification, no peak is observed in DTG curves, which suggests that the strictly gasification processes are not yet relevant in the experiments. Thermogravimetric studies between 800 °C and 1100 °C would be highly advisable.

- **Combustion**

In combustion, a much more intense degradation of lignocellulosic compounds occurs, although the first phases are closely related to pyrolysis, which is more explosive, even to the point of not correctly differentiating the peaks of hemicellulose and cellulose destruction in superior heating rates. Some characteristics of this process studied were the T_{ig} (ignition temperature), $T_{p,max}$ (temperature at which the greatest mass loss occurs, maximum peak DTG curve), $T_{p,max2}$ (temperature peak in the char combustion zone) and T_b (burn out temperature) [44]. In the thermogravimetric curve and even more so in the derived curve, two clearly areas of mass loss are observed (Fig. 2D). The heating and pyrolysis of *L. leucocephala* occur in the first zone, including the ignition and release of volatile compounds, which begins around 255 °C (T_{ig}). In this first zone, maximum degradation peaks ($T_{p,max}$) were observed in 314, 321, 327, 334 and 342 °C, to 5, 10, 15, 20 and 25 °C min^{-1}, respectively, with higher degradation rates than in pyrolysis and gasification (7.4, 17.8, 23.1, 30.8 and 31.7% min^{-1}) but at lower temperatures which could be the result of diffusion effects of pyrolytic evolution gases [45]. The second zone is based on the oxidation of the char and tar remaining after the loss of the volatiles in the biomass, diffusing the oxygen through the pores and producing combustion [46]. For the combustion zone, peaks ($T_{p,max2}$) were recorded in 424, 425, 438, 435 and 442 °C, to 5, 10, 15, 20 and 25 °C min^{-1}, respectively, degrading highs of 3.1, 11.0, 9.6, 10.4 and 9.8% min^{-1}. For L. *leucocephala*, a burn out temperature of 438, 443, 459, 472 and 487 °C, to 5, 10, 15, 20 and 25 °C min^{-1}, respectively.

3.1.3. Kinetic analysis with distributed activation energy model (DAEM)

To obtain a theoretical basis for the behavior of pyrolysis, gasification and combustion of *L. leucocephala*, a kinetic analysis was performed. Solid-state reaction kinetic data are interesting in understanding energy production processes from biomass resources. By

means of TGA, the main reaction zones of each thermochemical process can be distinguished and thus the kinetics of these processes can be analyzed in a simple way. Fig. 3 shows the Arrhenius graphs for the four thermochemical processes (A) Pyrolisys, B) 0.25 ER Gasification, C) 0.50 ER Gasification and D) Combustion) from which the activation energies for each conversion are calculated. In these graphs it can begin to distinguish how pyrolysis and gasification processes are kinetically similar with a greater inclination when the reaction progresses, that is, higher activation energy. Other aspects were also observed, for example, the oxidation zone of the remaining char in the combustion process with a conversion of 0.70 with a wider gap or the peaks of maximum biomass degradation when the lines almost overlap each other in all thermochemical treatments.

The numerical values of the activation energy are collected in Table 1 and represented in Fig. 4 at different conversions to better visualize certain aspects to be highlighted.

- **Pyrolysis**

Pyrolysis is divided into three zones, between 0.05 and 0.25 the degradation of hemicelluloses stands out with an average activation energy of 161 kJ mol^{-1} close to values reported for hemicellulose isolated bamboo that resulted in 167 kJ mol^{-1} [47], followed by a wide zone of cellulose breakdown and a certain amount of lignin between 0.25 and 0.65 with an activation energy of approximately 176 kJ mol^{-1}, close to studies recent for pine wood that obtained 180 kJ mol^{-1} [31]. And, finally, the slow and complex destruction of lignin structures occurs with a peak activation energy of 455 kJ mol^{-1} at a conversion rate of 0.9, corresponding to the area of most difficult degradation of all experiences, similar to recent own studies [48].

- **Gasification**

With regard to 0.25 ER gasification, the amount of oxygen introduced is so small that there are hardly any differences with pyrolysis throughout the degradation rate. Even so, small fluctuations in the activation energy are detected at interesting specific points such as the beginning of cellulose volatilization (V/V* of 0.30), since the activation energy is reduced from 170 to 152 kJ mol^{-1}, and at lignin destruction peak (V/V* of 0.90), where the activation energy is slightly lower (425 kJ mol^{-1} instead 455 kJ mol^{-1} in the case of pyrolysis). This implies that, although in a very low proportion, oxygen interferes with the volatilization of certain compounds, changing the reaction mechanisms. The 0.50 ER gasification has enough oxygen to detect more complex reactions based on the fact

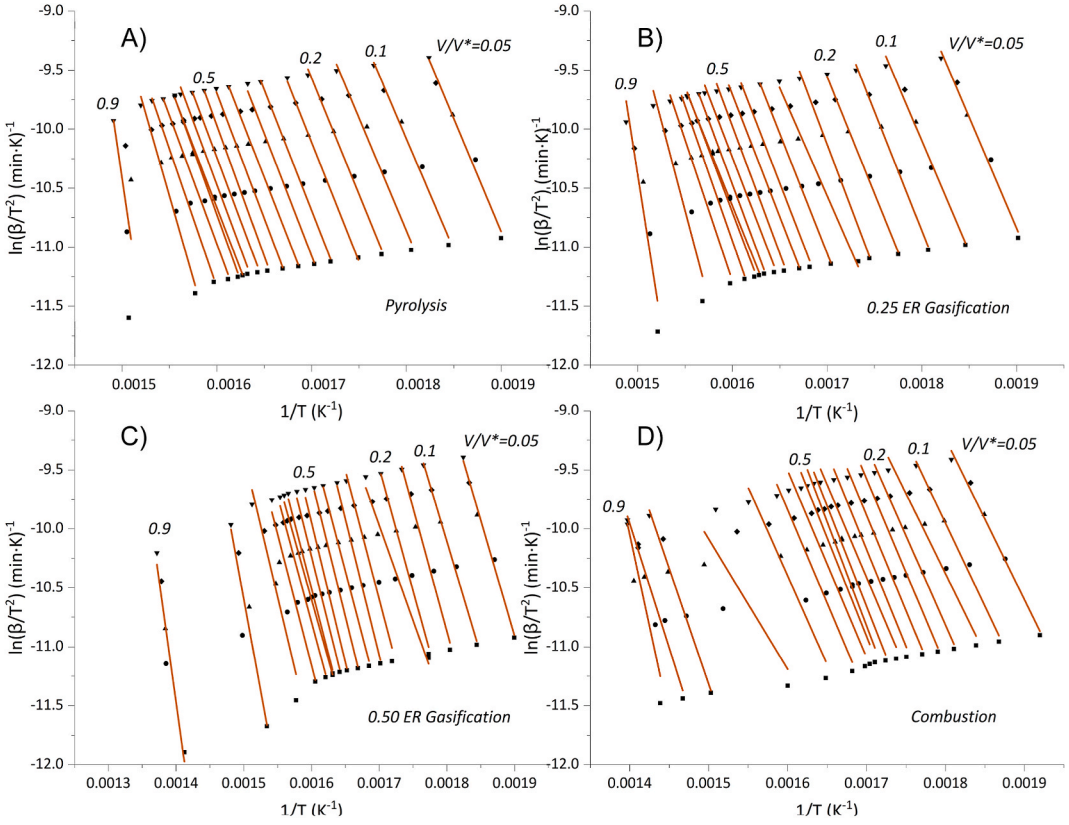

Fig. 3. Arrhenius plot of β/T^2 versus 1/T for each value of V/V* for different thermochemical processes: A) Pyrolisys, B) 0.25 ER Gasification, C) 0.50 ER Gasification and D) Combustion (▼ 25 °C min^{-1}, ◆ 20 °C min^{-1}, ▲ 15 °C min^{-1}, ● 10 °C min^{-1}, ■ 5 °C min^{-1}).

Table 1
Activation energies of *L. leucocephala* at specific conversion rate V/V* estimated applying the DAEM method.

	Leucaena leucocephala							
	Pyrolysis		0.25 ER Gasification		0.50 ER Gasification		Combustion	
V/V*	E_a (KJ mol^{-1})	R^2	E_a (KJ mol^{-1})	R^2	E_a (KJ mol^{-1})	R^2	E_a (KJ mol^{-1})	R^2
0.05	159.26	0.989	156.39	0.990	162.93	0.994	113.24	0.991
0.1	156.46	0.990	156.64	0.987	159.29	0.997	116.96	0.993
0.15	158.96	0.988	168.26	0.996	174.30	0.982	113.14	0.979
0.2	163.56	0.994	164.66	0.997	173.14	0.990	125.89	0.992
0.25	167.83	0.998	176.59	0.990	133.92	0.980	131.99	0.987
0.3	170.29	0.998	151.94	0.988	181.23	0.975	134.37	0.989
0.35	172.27	0.993	168.68	0.996	191.80	0.994	136.58	0.981
0.4	171.26	0.995	172.85	0.989	181.52	0.994	130.87	0.972
0.45	176.72	0.998	172.47	0.996	192.51	0.995	141.60	0.986
0.5	184.14	0.992	179.48	0.990	196.90	0.989	146.60	0.952
0.55	178.38	0.991	173.85	0.989	190.53	0.991	138.92	0.943
0.6	179.40	0.989	180.06	0.994	184.59	0.991	131.76	0.959
0.65	173.63	0.995	166.17	0.998	169.96	0.994	131.26	0.982
0.7	185.25	0.992	177.27	0.992	176.39	0.984	124.79	0.956
0.75	180.61	0.992	190.47	0.997	184.12	0.966	91.80	0.587
0.8	194.41	0.996	198.78	0.986	200.22	0.929	162.93	0.988
0.85	231.78	0.989	251.76	0.935	260.01	0.888	175.22	0.982
0.9	455.01	0.794	425.31	0.907	342.52	0.935	257.54	0.855

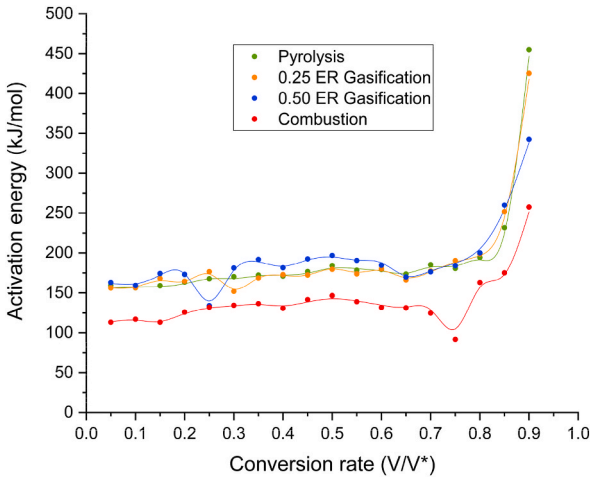

Fig. 4. Distribution of activation energies versus the conversion rate (V/V*) in the different thermochemical treatments applied to *L. leucocephala.*

that the activation energies are higher than in pyrolysis and 0.25 ER gasification, which indicates that not only ruptures of lignocellulosic structures occur in that zone, but also more complex recombination reactions with the oxygen involved. The first volatilization zone (V/V* of 0.05–0.20), mainly hemicellulose, has a lightly higher activation energy than in pyrolysis and 0.25 ER gasification, with a value of 167 kJ mol^{-1}. But, in the moment when the rupture of the first cellulose structures begins, the oxygen in the ambience considerably reduces the activation energy until 134 kJ mol^{-1} (V/V* of 0.25). However, the average activation energy along the main decomposition zone of cellulose together with lignin (V/V* of 0.30–0.65) is appreciably higher with an estimation of 186 kJ mol^{-1}. The last zone of decomposition of *L. leucocephala* in 0.50 ER gasification process, this study discerns a peak of activation energy of 343 kJ mol^{-1}, which agrees with data from complex char gasification reactions such as the partial oxidation of char with an oxygen-deficient atmosphere (2 C + O_2 ⇆ 2 CO) and the Boudouard reaction with carbon dioxide found in the evolution gases during volatilization (C + CO_2 ⇆ 2 CO), normally above 750 °C [39]. When temperatures are higher than 700 °C, gas-char gasification reactions are endothermic and tend to form synthesis gas (CO + H_2) with lower activation energies than pyrolysis [49].

- **Combustion**

As far as combustion is concerned, this process is significantly different from previous, although the first reaction zone is quite similar. The first zone of release light volatile compound, whose activation energy is 120 kJ mol^{-1} (V/V* = 0.05–0.25), is the ignition zone. Afterward, the cellulose and part of the less complex lignin devolatilization zone are located (V/V* = 0.25–0.65) with an activation energy of 136 kJ mol^{-1}, value that does not differ much from other combustion studies such as rice husk combustion with

142 kJ mol^{-1} [40]. The char and tar, one all the volatile material is released, allows oxygen to pass through its porous structure, oxidizing rapidly and exothermically. This zone (V/V* = 0.05–0.25) has an average activation energy of 107 kJ mol^{-1} highlighting a peak low of 92 kJ/mol. The combustion of tars and recalcitrant carbon compounds (V/V* = 0.8–0.85) obtains an average activation energy of 169 kJ mol^{-1} and peak degradation combustion lignin structures at V/V* = 0.9 of 258 kJ mol^{-1} close to burn out temperature. Combustion is a much simpler process to initiate kinetically and destroys biomass almost entirely, generating water, carbon dioxide and oxides such as sulfur or volatile metals, leaving inorganic ash as a solid residue.

3.2. Gasification-gas chromatography-mass spectrometry (Ga-GC/MS) study of L. leucocephala

Volatile organic products obtained by 0.25 ER and 0.50 ER gasification of *L. leucocephala* and analyzed by TD-GC/MS was listed in Table 2.

Interesting data and significant variations were noticed when distinguish between different equivalence ratios in the gasification and with respect to the compound obtained in pyrolytic process without oxidant atmosphere obtained in recent own studies [48].

For the gasification, noteworthy amount of hexane can be detected in the products from both 0.25 ER and 0.50 ER gasification. 0.25 ER gasification process can release 7.00% of hexane, while his contribution to 0.50 ER gasification is much more prominent with 44.96% giving the latter more capacity to produce quality bio-oil. 0.25 ER gasification shows a range of short-chain compounds

Table 2
Gas Chromatography-Mass Spectrometry (TD-GC/MS) products of *L. leucocephala* in two distinct gasification atmospheres (0.25 ER and 0.50 ER).

Compound	Formula	MW	*L. leucocephala*			
			0.25 ER gasification		0.50 ER gasification	
			Ret. Time (min)	Area (%)	Ret. Time (min)	Area (%)
Acetic acid	$C_2H_4O_2$	60.05	4.03	7.64		
Butane-2,3-dione	$C_4H_6O_2$	86.09	4.07	11.82		
Hexane	C_6H_{14}	86.18	4.16	7.00	4.16	44.96
2-methylpropan-1-ol	$C_4H_{10}O$	74.12			4.36	7.02
1-hydroxypropan-2-one	$C_3H_6O_2$	74.08	4.75	19.48	4.73	7.38
2,3-dihydro-1,4-dioxine	$C_4H_6O_2$	86.09	5.38	2.07		
Pyridine	C_5H_5N	79.10	6.22	2.34		
1-propan-2-yloxypropan-2-one	$C_6H_{12}O_2$	116.16	6.70	3.17		
Methyl 2-oxopropanoate	$C_4H_6O_3$	102.09	7.27	4.21		
Furan-2-carbaldehyde	$C_5H_4O_2$	96.08	8.84	4.59		
1-(4,6-dimethoxy-2,3-dimethylphenyl)ethanone	$C_{12}H_{16}O_3$	208.25			12.63	1.03
2-(2-hydroxyethoxy)ethanol	$C_4H_{10}O_3$	106.12			12.95	0.54
2-propylpentan-1-ol	$C_8H_{18}O$	130.23			14.92	0.66
Oxolan-2-ylmethanol	$C_5H_{10}O_2$	102.13			15.84	0.72
1-phenylethanone	C_8H_8O	120.15			16.06	0.57
2-methoxyphenol	$C_7H_8O_2$	124.14	16.64	0.91	16.62	0.23
Pentanal	$C_5H_{10}O$	86.13	16.72	1.90	16.71	1.06
Benzoic acid	$C_7H_6O_2$	122.12	18.16	1.07	18.15	1.31
5-(hydroxymethyl)oxolan-2-one	$C_5H_8O_3$	116.11			18.81	0.87
Benzene-1,2-diol	$C_6H_6O_2$	110.11	18.94	1.75	18.93	0.65
1,4:3,6-Dianhydro-.alpha.-D-glucopyranose	$C_6H_8O_4$	144.12	19.34	1.12	19.33	0.66
Sucrose	$C_{12}H_{22}O_{11}$	342.30	20.13	1.66	20.10	0.76
2,6-dimethoxyphenol	$C_8H_{10}O_3$	154.16	22.11	3.22	22.09	1.28
3-hydroxy-4-methoxybenzaldehyde	$C_8H_8O_3$	152.15			23.03	0.47
4-hydroxy-3-methoxybenzaldehyde	$C_8H_8O_3$	152.15	23.04	0.80		
4-hydroxy-3-methoxybenzoic acid	$C_8H_8O_4$	168.15	23.77	2.00	23.76	0.92
D-Allose	$C_6H_{12}O_6$	180.16	24.33	5.50	24.29	4.12
1-(3-hydroxy-4-methoxyphenyl)ethanone	$C_9H_{10}O_3$	166.17	24.52	0.82		
2-[2-[2-(2-hydroxyethoxy)ethoxy]ethoxy]ethanol	$C_8H_{18}O_5$	194.23			24.62	0.50
5-*tert*-butylbenzene-1,2,3-triol	$C_{10}H_{14}O_3$	182.23	25.08	1.30	25.07	0.61
1-(3-methoxy-4-propan-2-yloxyphenyl)propan-2-one	$C_{13}H_{18}O_3$	222.28	25.23	2.09	25.21	0.95
Propan-2-yl hexanoate	$C_9H_{18}O_2$	158.24	25.31	1.48	25.29	0.77
3,5-ditert-butyl-4-formylbenzoic acid	$C_{16}H_{22}O_3$	262.34			25.47	7.21
6-(5,6,7,8-tetrahydronaphthalen-2-yl)-1,2,3,4-tetrahydronaphthalene	$C_{20}H_{22}$	262.38	25.64	1.48	25.65	7.58
1-(3,5-dimethoxyphenyl)ethanone	$C_{10}H_{12}O_3$	180.20	25.70	1.20	25.69	0.81
Diethyl benzene-1,2-dicarboxylate	$C_{12}H_{14}O_4$	222.24			26.16	0.79
4-hydroxy-3,5-dimethoxybenzaldehyde	$C_9H_{10}O_4$	182.17	27.18	0.79	27.17	0.49
2,6-dimethoxy-4-prop-2-enylphenol	$C_{11}H_{14}O_3$	194.23	27.73	1.64	27.72	0.71
1-(4-hydroxy-3,5-dimethoxyphenyl)ethanone	$C_{10}H_{12}O_4$	196.20	28.24	0.76		
3-(4-hydroxy-3-methoxyphenyl)prop-2-enal	$C_{10}H_{10}O_3$	178.18	28.30	0.83		
1-(2,6-dihydroxy-4-methoxyphenyl)butan-1-one	$C_{11}H_{14}O_4$	210.23	28.74	2.39	28.72	0.94
2-[2-[2-[2-(2-hydroxyethoxy)ethoxy]ethoxy]ethoxy]ethanol	$C_{10}H_{22}O_6$	238.28			28.83	0.27
Methyl hexadecanoate	$C_{17}H_{34}O_2$	270.45			30.56	1.02
Pentadecanoic acid	$C_{15}H_{30}O_2$	242.40	31.01	2.15	31.00	2.13
Methyl octadecanoate	$C_{19}H_{38}O_2$	198.51	33.02	0.80		

compared to 0.50 ER gasification such as acetic acid (7.64%) produced by hemicellulose and cellulose degradation [50], dioxins (2.07%), pyridine (2.34%), derived of pyruvate (methyl 2-oxopropanoate) (4.21%), furan-2-carbaldehyde (furfural) (4.59%) mainly produced from the xylan units [51] or pentanal (1.90%), which disappear by interactions with higher amount of oxygen in 0.50 ER gasification originating carbon dioxide and water predominantly. The same behaviour follows the ketones that are widely detected in 0.25 ER gasification with more than 30% of total products, mainly 1-hydroxypropan-2-one (19.48%), butane-2,3-dione (11.82%) and 1-propan-2-yloxypropan-2-one (3.17%), which decreased to less than 10% in 0.50 ER gasification, being the compound that best tolerates the increase in oxygen the 1-hydroxypropan-2-one (7.38%) and shown other complex ketones such as 5-(hydroxymethyl) oxolan-2-one (0.87%). As can be observed, 1-hydroxypropan-2-one will be obtained in bioliquids in sufficient quantity to justify its separation and, thanks to its unique molecular structure, it is an essential intermediate and part of numerous products from the pharmaceutical industry, pesticides, pigments or fragrances [52].

Moreover, the gasification decomposition at 0.50 ER of *L. leucocephala* produce various alcohol compounds (8.99%), highlighting 2-methylpropan-1-ol (7.02%). Other interesting alcohols that are detected in the 0.50 ER gasification are simple polyglycols, for example, 2-(2-hydroxyethoxy)ethanol (diethylene glycol, 0.54%) and longer chains such as 2-[2-[2-(2-hydroxyethoxy)ethoxy]ethoxy] ethanol (tetra ethylene glycol, 0.50%) and 2-[2-[2-[2-(2-hydroxyethoxy)ethoxy]ethoxy]ethoxy]ethanol (pentaethylene glycol, 0.27%). These compounds are used extensively as antifreeze, lubricants, and specified solvents in the chemical industry [53]. As a result of the destruction of hemicellulose and cellulose, volatile saccharides compounds are detected, the total amount of which does not change significantly between the different gasification processes, even pyrolysis, with 8.28% for 0.25 ER gasification, 5.54% for 0.50 ER gasification and 5.10% for pyrolysis of *L. leucocephala* [48]. One aspect that does change is its composition, since for pyrolysis there was mainly glucopyranose (2.22%) followed by mannose and galactose, and in gasification, allose (5.50% and 4.12% in 0.25 ER and 0.50 ER gasification, respectively) stans out, closely followed by sucrose. D-allose is also one of the most relevant tar compounds in other gasification of biomass studies such as pine sawdust [54].

The compounds derived from the destruction of lignin were clearly the most detected in pyrolysis of *L. leucocephala*, however, in gasification, although lignin compounds were also detected (21.58% and 17.38% for 0.25 ER gasification and 0.50 ER gasification, respectively), its do so to a clearly much lesser extend (52.49% for pyrolysis). In gasification, ketones and alcohols lignin derived are found in greater proportion compared to pyrolysis, which guaiacol and syringol units were in more important extension [48]. Finally, it is necessary to comment on the detection of certain polycyclic aromatic products that make us realize the start of gasification reactions and destruction of the fixed carbon structures of the biomass, giving rise to 6-(5,6,7,8-tetrahydronaphthalen-2-yl)-1,2,3,4-tetrahydronaphthalene (1.48% and 7.58% for 0.25 ER gasification and 0.50 ER gasification, respectively). These heavy carbon products at higher temperatures and with the presence of carbon dioxide and other gas compounds will form synthesis gas ($CO + H_2$) under the right conditions. This compound is the most representative high tar product in *L. leucocephala* gasification process, and it consists of two united aromatic rings cyclically linked to a cyclohexane ring that are joined together by a C–C bond in aromatic carbon. These types of compounds are taken as references for the formation of tar and in its quantification in biomass gasification processes, as in the case of naphthalene [55].

4. Conclusions

The study infers that both gasification and pyrolysis can be used to obtain quality biofuels and chemicals and for industry from leguminous biomass without excessive variations in terms of energy. For *L. leucocephala*, it was shown that by introducing small amounts of oxygen into the system, the activation energy is reduced at the beginning of the destruction of hemicellulose and cellulose. Typical activation energies of the gasification process at a conversion rate of 0.8–0.9, which promotes the Boudouard reaction and partial oxidation of carbon. High amount of hexane as the primary alkane by-product was remarked in the 0.50 ER gasification, while short chain compounds highlighted in the case of 0.25 ER gasification. Higher amount of oxygen results in an increase of alcohols and ketones production. Glycols compounds are produced when the amount of oxygen is enough, and it was observed for 0.50 ER gasification process. Therefore, *L. leucocephala* is a valid material to generate a wide range of chemicals with the potential to produce second generation biofuels.

Author contribution statement

S. Clemente-Castro: Performed the experiments; Analyzed and interpreted the data.
A. Palma: Performed the experiments; Analyzed and interpreted the data; Wrote the paper.
M. Ruiz-Montoya: Conceived and designed the experiments; Analyzed and interpreted the data.
I. Giráldez: Analyzed and interpreted the data; Contributed reagents, materials, analysis tools or data.
M.J Díaz: Conceived and designed the experiments; Analyzed and interpreted the data; Contributed reagents, materials, analysis tools or data.

Data availability statement

Data will be made available on request.

Additional information

No additional information is available for this paper.

Declaration of competing interest

The authors declare that they have no known competing financial interests or personal relationships that could have appeared to influence the work reported in this paper.

Acknowledgments

This study was supported by the Ministry of Economy and Competitiveness (Spain), as well as by the National Research Program Oriented to the Challenges of Society (Project PID2020-112875RB-C21 funded by MCIN/AEI /10.13039/501100011033, t)he Ministry of Innovation, Science and Business of the Government of the Junta of Andalusia (Spain), the Operative Program is framed within FEDER Andalusia 2014–2020 with Project number UHU-125540, and the CEPSA Foundation Chair. Funding for open access charge: Universidad de Huelva / CBUA.

References

[[1] IPCC, AR6 Synthesis Report, Climate Change 2022, 2022, p. 7. https://www.ipcc.ch/report/sixth-assessment-report-cycle/.
[2] IEA, Net Zero by 2050, 2021, https://doi.org/10.1787/c8328405-en. Net Zero by 2050.
[3] A. Gasparatos, P. Stromberg, K. Takeuchi, Sustainability impacts of first-generation biofuels, Anim. Front. 3 (2013) 12–26, https://doi.org/10.2527/af.2013-0011.
[4] S. Bahri, U. Basak, S. Upadhyayula, Rational design of process parameters for carbon-neutral and sulfur-free motor fuel production from second-generation biomass generated syngas, J. Clean. Prod. 279 (2021), 123559, https://doi.org/10.1016/j.jclepro.2020.123559.
[5] United Nations, Energy Statistics Pocketbook, United Nation Publ., 2021, p. 78. https://unstats.un.org/unsd/energy/pocket/2018/2018pb-web.pdf.
[6] H.C. Ong, W.H. Chen, Y. Singh, Y.Y. Gan, C.Y. Chen, P.L. Show, A state-of-the-art review on thermochemical conversion of biomass for biofuel production: a TG-FTIR approach, Energy Convers. Manag. 209 (2020), https://doi.org/10.1016/j.enconman.2020.112634.
[7] H.H. Mardhiah, H.C. Ong, H.H. Masjuki, S. Lim, Y.L. Pang, Investigation of carbon-based solid acid catalyst from Jatropha curcas biomass in biodiesel production, Energy Convers. Manag. 144 (2017) 10–17, https://doi.org/10.1016/j.enconman.2017.04.038.
[8] H.B. Goyal, D. Seal, R.C. Saxena, Bio-fuels from thermochemical conversion of renewable resources: a review, Renew. Sustain. Energy Rev. 12 (2008) 504–517, https://doi.org/10.1016/j.rser.2006.07.014.
[9] T. Kan, V. Strezov, T.J. Evans, Lignocellulosic biomass pyrolysis: a review of product properties and effects of pyrolysis parameters, Renew. Sustain. Energy Rev. 57 (2016) 1126–1140, https://doi.org/10.1016/j.rser.2015.12.185.
[10] D. Chen, K. Cen, Z. Gan, X. Zhuang, Y. Ba, Comparative study of electric-heating torrefaction and solar-driven torrefaction of biomass: characterization of property variation and energy usage with torrefaction severity, Appl. Energy Combust. Sci. 9 (2022), 100051, https://doi.org/10.1016/j.jaecs.2021.100051.
[11] A.T. Hoang, H.C. Ong, I.M.R. Fattah, C.T. Chong, C.K. Cheng, R. Sakthivel, Y.S. Ok, Progress on the lignocellulosic biomass pyrolysis for biofuel production toward environmental sustainability, Fuel Process. Technol. 223 (2021), https://doi.org/10.1016/j.fuproc.2021.106997.
[12] S.H. Choi, V.I. Manousiouthakis, On the carbon cycle impact of combustion of harvested plant biomass vs. fossil carbon resources, Comput. Chem. Eng. 140 (2020), https://doi.org/10.1016/j.compchemeng.2020.106942.
[13] Z.R. Gajera, K. Verma, S.P. Tekade, A.N. Sawarkar, Kinetics of co-gasification of rice husk biomass and high sulphur petroleum coke with oxygen as gasifying medium via TGA, Bioresour. Technol. Reports. 11 (2020), https://doi.org/10.1016/j.biteb.2020.100479.
[14] J.L. Zheng, M.Q. Zhu, J.L. Wen, R. cang Sun, Gasification of bio-oil: effects of equivalence ratio and gasifying agents on product distribution and gasification efficiency, Bioresour. Technol. 211 (2016) 164–172, https://doi.org/10.1016/J.BIORTECH.2016.03.088.
[15] Z. Yang, Y. Wu, Z. Zhang, H. Li, X. Li, R.I. Egorov, P.A. Strizhak, X. Gao, Recent advances in co-thermochemical conversions of biomass with fossil fuels focusing on the synergistic effects, Renew. Sustain. Energy Rev. 103 (2019) 384–398, https://doi.org/10.1016/j.rser.2018.12.047.
[16] H. Liu, M.S. Ahmad, H. Alhumade, A. Elkamel, S. Sammak, B. Shen, A hybrid kinetic and optimization approach for biomass pyrolysis: the hybrid scheme of the isoconversional methods, DAEM, and a parallel-reaction mechanism, Energy Convers. Manag. 208 (2020), https://doi.org/10.1016/j.enconman.2020.112531.
[17] Q.H. Ng, B.L.F. Chin, S. Yusup, A.C.M. Loy, K.Y.Y. Chong, Modeling of the co-pyrolysis of rubber residual and HDPE waste using the distributed activation energy model (DAEM), Appl. Therm. Eng. 138 (2018) 336–345, https://doi.org/10.1016/j.applthermaleng.2018.04.069.
[18] K. Czajka, A. Kisiela, W. Moroń, W. Ferens, W. Rybak, Pyrolysis of solid fuels: thermochemical behaviour, kinetics and compensation effect, Fuel Process. Technol. 142 (2016) 42–53, https://doi.org/10.1016/j.fuproc.2015.09.027.
[19] D. Madayi, P.H. Surya, K.K. Elyas, A Glucose binding lectin from Leucaena leucocephala seeds and its mitogenic activity against human lymphocytes, Int. J. Biol. Macromol. 163 (2020) 431–441, https://doi.org/10.1016/j.ijbiomac.2020.07.025.
[20] N.C.P. Bomfim, J.V. Aguilar, W. da S. de Paiva, L.A. de Souza, G.C. Justino, G.A. Faria, L.S. Camargos, Iron phytostabilization by Leucaena leucocephala, South Afr. J. Bot. 138 (2021) 318–327, https://doi.org/10.1016/j.sajb.2021.01.013.
[21] C.E.L. Lins, U.M.T. Cavalcante, E.V.S.B. Sampaio, A.S. Messias, L.C. Maia, Growth of mycorrhized seedlings of Leucaena leucocephala (Lam.) de Wit. in a copper contaminated soil, Appl. Soil Ecol. 31 (2006) 181–185, https://doi.org/10.1016/j.apsoil.2005.06.004.
[22] M. Ruiz-Montoya, A. Palma, S. Lozano-Calvo, E. Morales, M.J. Díaz, Kinetic synergistic effect in co-pyrolysis of Eucalyptus globulus with high and low density polyethylene, Energy Rep. 8 (2022) 10688–10704, https://doi.org/10.1016/j.egyr.2022.08.200.
[23] J. Li, Y. Tian, P. Zong, Y. Qiao, S. Qin, Thermal cracking behavior, products distribution and char/steam gasification kinetics of seawater Spirulina by TG-FTIR and Py-GC/MS, Renew. Energy 145 (2020) 1761–1771, https://doi.org/10.1016/j.renene.2019.07.096.
[24] S. Yousef, J. Eimontas, N. Striūgas, M.A. Abdelnaby, Pyrolysis and gasification kinetic behavior of mango seed shells using TG-FTIR-GC–MS system under N2 and CO2 atmospheres, Renew. Energy 173 (2021) 733–749, https://doi.org/10.1016/j.renene.2021.04.034.
[25] TAPPI test method T 257 cm-02. Sampling and preparing wood for analysis, in: TAPPI Test Methods, Technical Association of the Pulp and Paper Industry., Atlanta, G.A, 2012.
[26] TAPPI Test Method T 249 cm-85. Carbohydrate composition of extractive-free wood and wood pulp by Gas-Liquid Chromatography, in: TAPPI Test Methods, Technical Association of the Pulp and Paper Industry., Atlanta, G.A, 1985.
[27] Fabrizio Scala, Fluidized Bed Technologies for Near-Zero Emission Combustion and Gasification, first ed., 2013.
[28] P. Palies, Stabilization and Dynamic of Premixed Swirling Flames: Prevaporized, Stratified, Partially, and Fully Premixed Regimes, Stab. Dyn. Premixed Swirling Flames Prevaporized, Stratif. Partial. Fully Premixed Regimes, 2020, pp. 1–378, https://doi.org/10.1016/C2019-0-00497-9.
[29] D.S. Upadhyay, A.K. Sakhiya, K. Panchal, A.H. Patel, R.N. Patel, Effect of equivalence ratio on the performance of the downdraft gasifier – an experimental and modelling approach, Energy 168 (2019) 833–846, https://doi.org/10.1016/J.ENERGY.2018.11.133.

[30] R. Xiao, W. Yang, X. Cong, K. Dong, J. Xu, D. Wang, X. Yang, Thermogravimetric analysis and reaction kinetics of lignocellulosic biomass pyrolysis, Energy 201 (2020), https://doi.org/10.1016/j.energy.2020.117537.
[31] C.N. Arenas, M.V. Navarro, J.D. Martínez, Pyrolysis kinetics of biomass wastes using isoconversional methods and the distributed activation energy model, Bioresour. Technol. 288 (2019), 121485, https://doi.org/10.1016/j.biortech.2019.121485.
[32] J. Cai, W. Wu, R. Liu, G.W. Huber, A distributed activation energy model for the pyrolysis of lignocellulosic biomass, Green Chem. 15 (2013) 1331–1340, https://doi.org/10.1039/c3gc36958g.
[33] J. Cai, T. Li, R. Liu, A critical study of the Miura-Maki integral method for the estimation of the kinetic parameters of the distributed activation energy model, Bioresour. Technol. 102 (2011) 3894–3899, https://doi.org/10.1016/j.biortech.2010.11.110.
[34] J. Cai, W. Wu, R. Liu, An overview of distributed activation energy model and its application in the pyrolysis of lignocellulosic biomass, Renew. Sustain. Energy Rev. 36 (2014) 236–246, https://doi.org/10.1016/j.rser.2014.04.052.
[35] T. Sonobe, N. Worasuwannarak, Kinetic analyses of biomass pyrolysis using the distributed activation energy model, Fuel 87 (2008) 414–421, https://doi.org/10.1016/j.fuel.2007.05.004.
[36] K. Miura, A new and simple method to estimate f(E) and ko(E) in the distributed activation energy model from three sets of experimental data, Energy Fuel. 9 (1995) 302–307, https://doi.org/10.1021/ef00050a014.
[37] S. Munir, S.S. Daood, W. Nimmo, A.M. Cunliffe, B.M. Gibbs, Thermal analysis and devolatilization kinetics of cotton stalk, sugar cane bagasse and shea meal under nitrogen and air atmospheres, Bioresour. Technol. 100 (2009) 1413–1418, https://doi.org/10.1016/j.biortech.2008.07.065.
[38] X. Yang, R. Zhang, J. Fu, S. Geng, J.J. Cheng, Y. Sun, Pyrolysis kinetic and product analysis of different microalgal biomass by distributed activation energy model and pyrolysis-gas chromatography-mass spectrometry, Bioresour. Technol. 163 (2014) 335–342, https://doi.org/10.1016/j.biortech.2014.04.040.
[39] A. Meng, S. Chen, Y. Long, H. Zhou, Y. Zhang, Q. Li, Pyrolysis and gasification of typical components in wastes with macro-TGA, Waste Manag. 46 (2015) 247–256, https://doi.org/10.1016/j.wasman.2015.08.025.
[40] K.G. Mansaray, A.E. Ghaly, Determination of kinetic parameters of rice husks in oxygen using thermogravimetric analysis, Biomass Bioenergy 17 (1999) 19–31, https://doi.org/10.1016/S0961-9534(99)00022-7.
[41] M. Radhakumari, D.J. Prakash, B. Satyavathi, Pyrolysis characteristics and kinetics of algal biomass using tga analysis based on ICTAC recommendations, Biomass Convers. Biorefinery. 6 (2016) 189–195, https://doi.org/10.1007/S13399-015-0173-7/FIGURES/5.
[42] G. Mishra, J. Kumar, T. Bhaskar, Kinetic studies on the pyrolysis of pinewood, Bioresour. Technol. 182 (2015) 282–288, https://doi.org/10.1016/j.biortech.2015.01.087.
[43] A. Ramos, E. Monteiro, A. Rouboa, Numerical approaches and comprehensive models for gasification process: a review, Renew. Sustain. Energy Rev. 110 (2019) 188–206, https://doi.org/10.1016/J.RSER.2019.04.048.
[44] J.J. Lu, W.H. Chen, Investigation on the ignition and burnout temperatures of bamboo and sugarcane bagasse by thermogravimetric analysis, Appl. Energy 160 (2015) 49–57, https://doi.org/10.1016/J.APENERGY.2015.09.026.
[45] R. Kaji, Y. Hishinuma, Y. Nakamura, Low temperature oxidation of coals: effects of pore structure and coal composition, Fuel 64 (1985) 297–302, https://doi.org/10.1016/0016-2361(85)90413-2.
[46] K. Jayaraman, I. Gökalp, Pyrolysis, combustion and gasification characteristics of miscanthus and sewage sludge, Energy Convers. Manag. 89 (2015) 83–91, https://doi.org/10.1016/J.ENCONMAN.2014.09.058.
[47] J. Zou, H. Hu, M.M. Rahman, D. Yellezuome, F. He, X. Zhang, J. Cai, Non-isothermal pyrolysis of xylan and lignin: a hybrid simulated annealing algorithm and pattern search method to regulate distributed activation energies, SSRN Electron. J. 187 (2022), 115501, https://doi.org/10.2139/ssrn.4059367.
[48] S. Clemente-Castro, A. Palma, M. Ruiz-Montoya, I. Giráldez, M.J. Díaz, Pyrolysis kinetic, thermodynamic and product analysis of different leguminous biomasses by Kissinger-Akahira-Sunose and pyrolysis-gas chromatography-mass spectrometry, J. Anal. Appl. Pyrolysis 162 (2022), https://doi.org/10.1016/j.jaap.2022.105457.
[49] F. Fantozzi, P. Bartocci, Integrated gasification combined cycle (IGCC) Technologies, Elsevier. http://www.sciencedirect.com:5070/book/9780081001677/integrated-gasification-combined-cycle-igcc-technologies?via=ihub=, 2017. (Accessed 2 March 2023).
[50] C. Font Palma, Modelling of tar formation and evolution for biomass gasification: a review, Appl. Energy 111 (2013) 129–141, https://doi.org/10.1016/j.apenergy.2013.04.082.
[51] D.K. Shen, S. Gu, A.V. Bridgwater, Study on the pyrolytic behaviour of xylan-based hemicellulose using TG–FTIR and Py–GC–FTIR, J. Anal. Appl. Pyrolysis 87 (2010) 199–206, https://doi.org/10.1016/J.JAAP.2009.12.001.
[52] H.J. Choe, K.H. Song, Liquid-liquid Equilibria for pseudo-ternary systems of 1-Hydroxypropan-2-one + water + cyclic terpene-based mixtures at 298.15 K, J. Chem. Eng. Data 68 (2023) 430–440, https://doi.org/10.1021/acs.jced.2c00737.
[53] A. Hayyan, M.K. Hadj-Kali, M.Z.M. Salleh, M.A. Hashim, S.R. Rubaidi, M. Hayyan, M.Y. Zulkifli, S.N. Rashid, M.E.S. Mirghani, E. Ali, W.J. Basirun, Characterization of tetraethylene glycol-based deep eutectic solvents and their potential application for dissolving unsaturated fatty acids, J. Mol. Liq. 312 (2020), https://doi.org/10.1016/j.molliq.2020.113284.
[54] X. Tian, P. Niu, Y. Ma, H. Zhao, Chemical-looping gasification of biomass: Part II. Tar yields and distributions, Biomass Bioenergy 108 (2018) 178–189, https://doi.org/10.1016/j.biombioe.2017.11.007.
[55] A. Horvat, M. Kwapinska, G. Xue, S. Dooley, W. Kwapinski, J.J. Leahy, Detailed measurement uncertainty analysis of solid-phase adsorption-total gas chromatography (GC)-Detectable tar from biomass gasification, Energy Fuel. 30 (2016) 2187–2197, https://doi.org/10.1021/acs.energyfuels.5b02579.